Mechanics of Advanced Composite Structures 6 (2019) 19–26

Semnan University

Mechanics of Advanced Composite Structures

journal homepage: http://MACS.journals.semnan.ac.ir

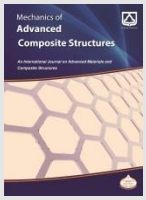

Health Monitoring for Composite Under Low-Cycle Cyclic Loading, Considering Effects of Acoustic Emission Sensor Type

M. Alizadeh [a], H. Sayar [a], M. Azadi [a*], S.M. Jafari [b]

[a] *Faculty of Mechanical Engineering, Semnan University, Semnan, P.O. Box: 35131-19111, Iran*
[b] *Faculty of Mechanical and Energy Engineering, Shahid Beheshti University, A.C., Tehran, P.O. Box: 16765-1719, Iran*

PAPER INFO

Paper history:
Received 2018-10-12
Received in revised form 2018-12-12
Accepted 2019-04-25

Keywords:
Health monitoring
Composite structure
Low-cycle cyclic loading
Acoustic emission
Sensor type

ABSTRACT

Composites have been widely used in the aerospace industry. Due to the requirement of a high safety for such structures, they could be considered for health monitoring. The acoustic emission approach is one of most effective methods for identifying damages in composites. In this article, standard specimens were made from carbon fibers and the epoxy resin, with the $[0_3/90_2/0_2]_s$ layout. Then, samples were subjected to low-cycle cyclic loading. Besides, signals were recorded with two types of acoustic emission sensors. Obtained results indicated that by increasing the number of cycles and approaching the final lifetime of the sample, the cumulative energy of signals increased. The fracture surface of specimens was analyzed using the scanning electron microscopy. As a consequent and a general conclusion, based on obtained results, it could be claimed that both wide-band and mid-band acoustic emission sensors could be effectively utilized for detecting the defects in composite structures.

1. Introduction

Various studies have been performed on health monitoring of composite structures. For such objective, the acoustic emission approach is one of the most effective methods for the damage detection in such components. In the following paragraphs, a literature review is presented in this regard.

Liu et al. [1] studied the effects of different layers and the size of the hole on the result of the acoustic emission method to find a relationship between failure characteristics and acoustic emission signal parameters including the energy, count and amplitude parameters. They also observed microscopic properties of different composite specimens after failure by the scanning the electron microscopy. Their research focused on damage mechanisms of the open-hole carbon fiber composite by combining the traction and the acoustic emission test. Mohammadi et al. [2] examined the relationship between the acoustic emission approach and the finite element method in the detection of damage mechanisms in the open-hole glass/epoxy composite under tensile loading. They utilized the wavelet packet transform and the fuzzy clustering for acoustic emission signal processing. They also examined failure mechanisms in samples. Their results showed that the difference between the finite element method and the wavelet packet transform approach was less than 15%. However, the difference was more than 42%, between the fuzzy clustering approach and the finite element method. In addition, they obtained the frequency range of the acoustic emission signals, in terms of a fast Fourier transform and then, they determined the frequency range of matrix cracking and the fiber breakage by testing each material, separately. The frequency range of matrix cracking was found as 80-250 kHz and the frequency range of the fiber breakage was 375-480 kHz. According to previous studies [3-4], the frequency range for debonding of the fibers from the

* Corresponding author. Tel.: +98-910-210-7280; Fax: +98-23-33321005
E-mail address: m_azadi@semnan.ac.ir

DOI: 10.22075/macs.2019.16157.1166

matrix was considered between those of matrix cracking and the failure in fibers, which was 250-375 kHz. Ni and Iwamoto [5] analyzed the acoustic emission signals with the wavelet packet transform in failure of composites. Their results showed that the fast Fourier transform and the wavelet packet transform could identify the fracture patterns in composite materials.

Loutas and Kostopoulos [6] investigated the behavior of carbon/epoxy composites under tension-tension fatigue loading. They used the acoustic emission approach to monitor the state of the test sample during loading. The threshold, which was chosen by them, was 40 dB. Nixon-Pearson et al. [7] conducted an experiment to observe and understand the developmental stages of the damage, throughout the lifetime of a quasi-isotropic open-hole carbon/epoxy composite laminate, which was loaded under tension-tension fatigue loading. Using the X-ray method, they examined the damage in three-dimensional specimens. Their results indicated that when the maximum fatigue stress increased, the number of cycles, which caused the specimen fracture, decreased linearly. Firstly, they subjected samples to obtain the mean resistance of materials under quasi-static loading. Then, they performed fatigue tests to determine the incidence of the peak-to-peak damage under 60% of the final static load, using the X-ray approach. Thermographic images showed that the initial damage began with matrix cracking and the delamination at the edge of the hole. Bourchak et al. [8] studied the energy of acoustic emission signals as a component of the fatigue damage for carbon fiber composites. Their acoustic emission results illustrated that the composite damage occurred at about 27% of the ultimate tensile strength and at 0.3% of the ultimate strain for composites with 90° layers. Williams and Reifsnider [9] investigated the boron-aluminum and boron-epoxy angle-plied composite specimens under strain- and load-controlled fatigue loading, using the acoustic emission method. They observed a good correlation between the percentage and the progress of the damage and also the results of the acoustic emission approach. They stated that depending on the type of the material, debonding of fibers from the matrix could create large signals. Mahdavi et al. [10] analyzed the failure of composite tubes, made by the filament method, using the acoustic emission approach. They examined some sections of glass tubes to get the tensile strength. They also analyzed several acoustic emission signal parameters, including the energy and the cumulative energy during the test. Their results indicated that the frequency range of matrix cracking and debonding of fibers from the matrix was 40-80 dB, the frequency range of the delamination was 80-90 dB and the frequency range of the fiber breakage was 90-94 dB. They utilized scanning electron microscopy images to find the mechanism of failures.

Sayar et al. [11] found damage mechanisms in the open-hole laminated carbon/epoxy composite, by the acoustic emission method. They investigated the clustering effect on the damage mechanism of composites. In addition, they categorized five damage mechanisms including matrix cracking, the fiber breakage, the fiber pull-out, debonding of fibers from the matrix and the delamination, by acquiring acoustic emission signals. Alizadeh et al. [12] studied the failure mechanisms in laminate composite specimens, under cyclic loadings at different displacement amplitudes, using the acoustic emission approach. They found the damage mechanisms based on three defects in open-hole tensile tests, under the low-cycle fatigue loading condition. Ghasemi-Ghalebahman et al. [13] studied different types of failure mechanisms in laminate composite specimens, under tensile loading at 2 mm/min of the loading rate, using the acoustic emission method. They calculated the percentage of various damage mechanisms. Azadi et al. [14] illustrated the effect of the tensile loading rate on mechanical properties and failure mechanisms in open-hole carbon fiber reinforced polymer composites using acoustic emission method. They indicated that by enhancement of the tensile loading rate, the maximum stress increased and the maximum strain decreased, in open-hole composite specimens. Besides, they found the frequency range of damage mechanisms. In another work, Azadi et al. [15] investigated the low-cycle fatigue lifetime and performed the sensitivity analysis to depict effects of the displacement amplitude and the loading frequency on the low-cycle fatigue lifetime in carbon/epoxy laminated composites. They showed that by enhancement of the displacement amplitude, the low-cycle fatigue lifetime decreased. In addition, when the loading frequency increased, the low-cycle fatigue lifetime of composites decreased. Besides, the maximum stress had a reverse trend, comparing to the fatigue lifetime. They illustrated that the displacement amplitude was sensitive to the fatigue lifetime and the maximum stress and the loading frequency was sensitive to the maximum stress and not to the fatigue lifetime.

As a result, from the literature review, it could be concluded that studies have rarely been performed on fatigue properties of carbon fiber/epoxy composites and their health monitoring with the acoustic emission approach. As a conclusion, it could be claimed that two aspects of novelty for this article are investigations of the material under cyclic load-

ing, especially in the low-cycle fatigue regime, and finding the influence of using acoustic emission sensor types on the detection of failures in carbon fiber/epoxy composite materials. Therefore, in this study, the low-cycle fatigue test was empirically discussed by analyzing acquired acoustic emission signals, during testing. Then, obtained results could be interpreted by referring to the figures.

2. Experimental Works

2.1. Materials and Tests

Composite samples were manufactures from the carbon fiber and the epoxy resin. The carbon fiber was from Sika Company with a specific gravity of 230 gr/m^2. The epoxy type was the CR-80 resin. At the first stage, a composite sheet was made with the dimension of 250 × 350 mm and the thickness of 3.2 mm, in the $[0_3/90_2/0_2]_s$ layout. This composite sheet was made by the hand lay-up method with compression molding. Then, standard specimens were cut from this sheet using the water-jet approach. The dimension of each composite sample was 3.2, 250 and 36 mm based on the thickness, the length and the width of samples, respectively. At the final stage, a 6 mm diameter hole was drilled in the center of all composite specimens, based on the ASTM D5766 standard [16].

The tensile test device, STM-150 from Santam Company, was utilized with a capacity of 15 tons and the adjustable loading capacity, ranging from 0.1 to 500 mm/min. Then, a sample was loaded in a tensile condition at 200 mm/min of the loading frequency and under 6.5 mm of the displacement amplitude.

2.2. Acoustic Emission Signals

The acoustic emission approach can be used according to the production of transient elastic waves in materials, during release of the energy, from an available source in the ultrasonic range, including the frequency of 1 kHz to 20 MHz [12]. Common parameters for acoustic emission signals, which are shown in Fig. 1, could be listed as follows:

1. Count: When the signal exceeds the defined threshold, a hit will be recorded.

2. Hit: The number of times that the signal exceeds the threshold during a period. It is worth mentioning that the counting index is fully set at the threshold and the operating frequency depends on this parameter.

3. Amplitude: The highest voltage of the signal is called "amplitude". In measurements of the acoustic emission approach, the amplitude is expressed in dB. The amplitude has the exact dependency on the source domain.

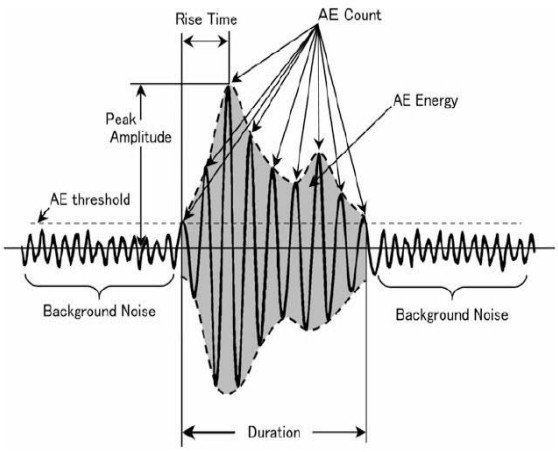

Fig. 1. Parameters of acoustic emission signals [19].

4. Duration: The interval between the first and last hit of acoustic emission signals. The duration depends on the source and the range of noise filters.

5. Rise time: It is the interval between the time of the first hit and the time determines the largest amount of signals. The rise time is the exact relationship with the source time function and the type of failures or the noise removal method.

6. Energy: In acoustic emission systems, the definition of the energy is identified by area below the graph. This parameter depends on the amplitude and duration of the signal [17].

The acoustic emission signal is usually amplified by the pre-amplifier and then filtering is performed on signals. The amplifier output is expressed in dB, as shown in Eq. (1), which means the ratio of the output voltage (v_o) to the input voltage (v_i) [20], as follows:

$$dB = 20\ log\ _{10}\left(\frac{v_o}{v_i}\right) \quad (1)$$

Eq. (2) shows the energy of the acoustic emission signal, which is calculated by the mean square value over the time [21], as below:

$$E = \int_0^t v^2(t)\,dt \quad (2)$$

in which, v is the amount of the voltage for the waveform of the acoustic emission method, t is the time, and E is the acoustic emission energy. As the source wavelength increases, the wave energy decreases exponentially, as shown in Eq. (3) [16].

$$E(x) = E_0 e^{-kx} \quad (3)$$

where E is the energy at the distance, x, from the source, E_0 is the source energy, k is the wavelength loss and x is the distance from the source.

2.3. Acoustic Emission Sensors and Equipments

In order to record the acoustic emission signals, two wide-band sensors were utilized with the oper-

ating frequency range of 100-1000 kHz. In addition, two mid-band sensors were also used with the operating frequency range of 200-750 kHz. They were installed on standard specimens. Acoustic emission signals were amplified 40 dB by two 2/4/6 preamplifiers. Then, data were recorded with 1 MHz of the sample rate and were saved by the PCI-2 analog-to-digital board and the AE-WIN software, from PAC Company. The threshold of acoustic emission signals was found to be 35 dB. In order to calibrate the sensors, the pencil lead break method was utilized, according to the ASTM-E976 standard [22]. It should be noted that a silicone grease was used for a proper contact of sensors to the specimen surface. Fig. 2 shows test equipments including cyclic loading equipments, the test sample, acoustic emission equipments and interface cables.

3. Results and Discussions

3.1. Low-cycle Cyclic Test Results

As mentioned in the previous section, the carbon/epoxy composite sample was loaded at the loading frequency of 200 mm/min and under the displacement amplitude of 6.5 mm. It should be noted that the test was performed under the displacement-controlled condition. Under such tensile cyclic loading condition, the low-cycle fatigue lifetime of this sample was obtained as 19 cycles. Then, other obtained results were normalized based on this value for the fatigue lifetime.

Fig. 3 shows the maximum stress and the minimum stress during cycles. Based on these results, the maximum stress was obtained as 593 MPa. This value was related to the first cycle. Then, the maximum stress reduced during testing. As another result, the minimum stress was near zero during all cycles.

3.2. Analysis of Acoustic Emission Data

In this section, the analysis of acoustic emission signals, which was mainly extracted from the energy parameter, is discussed. As the acoustic energy described, the higher number of the signal count exceeded the threshold value and higher acoustic energy would be produced.

Fig. 4 presents the maximum stress versus the normalized fatigue lifetime, besides the energy of acoustic emission signals for two types of sensors. This graph could be divided into three regions. In the first step, the acoustic energy increased during the first few cycles; and then, the acoustic energy decreased, and returned to an equilibrium state, until it reached to the final stage and the specimen failed. As final cycles reach, the fatigue phenomenon appeared to be associated with a sharp enhancement in the acoustic energy. As it can be seen, in the 19th cycle, the sample completely failed, where the failure caused to produce high acoustic energy. In this loading, due to the high amplitude of loading, the microscopic damage increased suddenly in the early cycles; and then, it entered to the macroscopic damage in final cycles. This behavior could be also distinguished from changes in the acoustic energy.

Fig. 5 shows the maximum stress versus the normalized fatigue lifetime, besides the cumulative energy of two types of sensors. The cumulative energy increased for two sensors with a small difference. This difference could be due to the operating frequency or the different location of two sensors. At the moment corresponding to the final failure, the cumulative energy of both sensors greatly increased, in which a good agreement between the cumulative energy and the maximum stress versus the normalized fatigue lifetime could be observed.

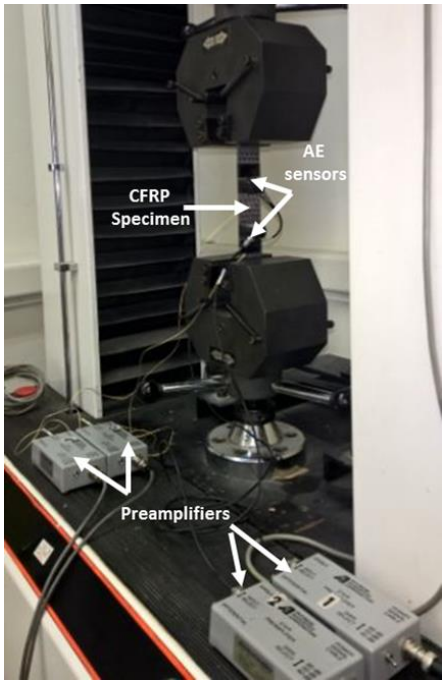

Fig. 2. Equipments of cyclic tensile testing and the acoustic emission approach.

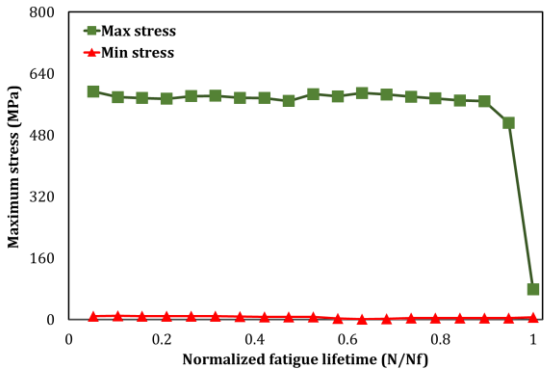

Fig. 3. The maximum stress and the minimum stress versus the normalized fatigue lifetime.

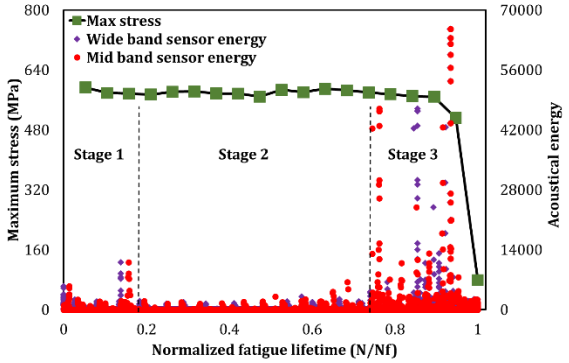

Fig. 4. The acoustical energy of two types of sensors and the maximum stres versus the normalized fatigue lifetime.

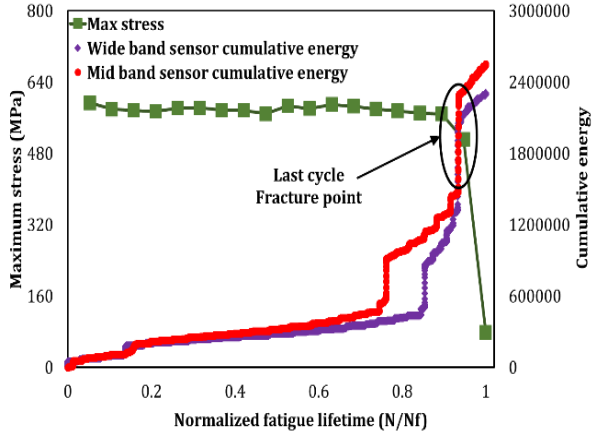

Fig. 5. The cumulative energy of two types of sensors and the maximum stress versys the normalized fatigue lifetime.

In Fig. 6, the diagram of the cyclic strain versus the normalized lifetime diagram was compared to the acoustical energy. The loading range in the test was constant and therefore, the strain range varied from zero to 0.43. As it can be seen, the energy of both sensors increased significantly in the last cycle, which was also mentioned for Fig. 4. This energy raise was due to the sudden failure of the composite sample.

Fig. 7 shows the count parameter of acoustic emission signals for two types of sensors, including the wide-band sensor and the mid-band sensor. Again, data were divided into three stages. The first stage, which is the beginning stage of loading and initial cycles, resulted in microscopic damages. According to this phenomenon, the number of counts increased. By approaching to the last cycle, due to a high damage value, a large number was counted by both sensors, which was consistent with the acoustical energy, which was discussed before in Fig. 4 and Fig. 6.

As a conclusion, both wide-band and mid-band sensors could effectively monitor the health of composite structures. There was a small difference between signals, obtained from two different sensors. Such results could be mentioned for the energy and the count parameter. However, in the cumulative energy, there was a difference between two sensors, which the mid-band sensor predicted damages in an earlier time duration, from about 70% of the fatigue lifetime, in comparison to that of the wide-band sensor.

Obtained results in this research could be compared to results of other studies on the crack initiation and the crack growth in metals. In such studies [23-25], researchers found the fatigue crack propagation in metals by acoustic emission signals. These results could verify the results of this research for composites. In addition, Ma and Li [26] utilized the acoustic emission technique to assess and monitor the damage in the fiber reinforced polymer-strengthened reinforced concrete columns under cyclic loading. They indicated that the cumulative acoustic emission energy would exhibit a good correlation with the cumulative hysteretic energy, dissipated during cyclic testing. In order to verify the obtained results in this article, it could be claimed that the cumulative energy could predict the crack initiation and the crack propagation in composites, the same as reported in the literature [26].

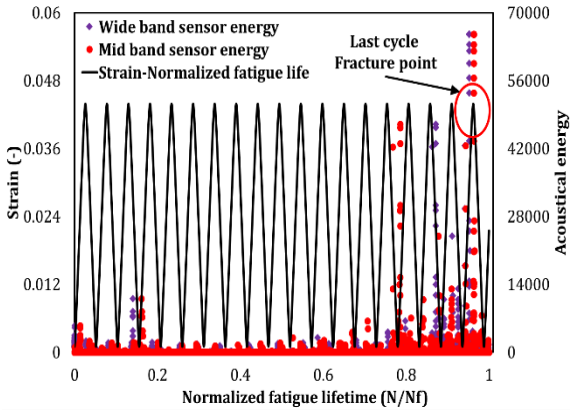

Fig. 6. The acoustical energy of two types of sensors and the strain versus the normalized fatigue lifetime.

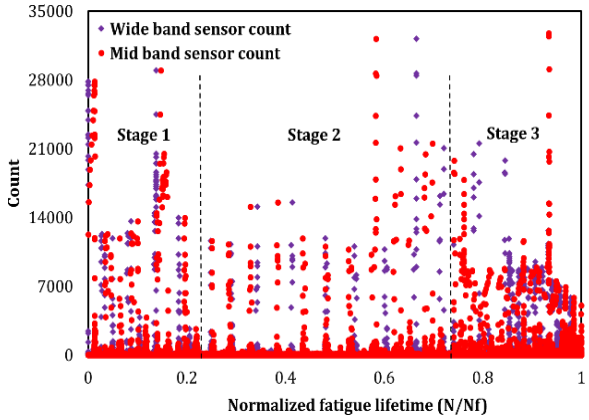

Fig. 7. The acount parameter of two types of sensors.

3.3. Scanning Electron Microscopy Images

The scanning electron microscopy was utilized to observe the failure mechanisms of the composite specimen. Images were taken from the surface of the fracture and surrounding the hole, in which higher stress concentration occurred. In Fig. 8, fibers in the sample were well characterized in two layers, including 0 and 90° layers.

In the 0° layer, the matrix cracking, the fiber breakage and debonding of fibers from the matrix occurred as damage mechanisms; while in the 90° layer, due to the fact that the loading direction was perpendicular to the direction of the fibers, the failure of fibers occurred much less than that of the 0° layer. The most failure mechanism for the 90° layer was matrix cracking and debonding of fibers from the matrix.

Fig. 9 shows the matrix cracking, debonding of fibers from the matrix and the fiber breakage, as damage mechanisms, with higher magnification in comparison to Fig. 8. In addition, for such defects, higher magnification of the mentioned image can be also observed in Fig. 10.

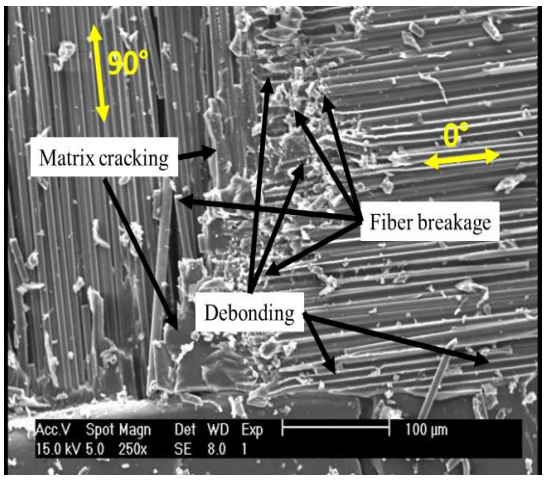

Fig. 8. The scanning electron microscopy image for 0 and 90° layers.

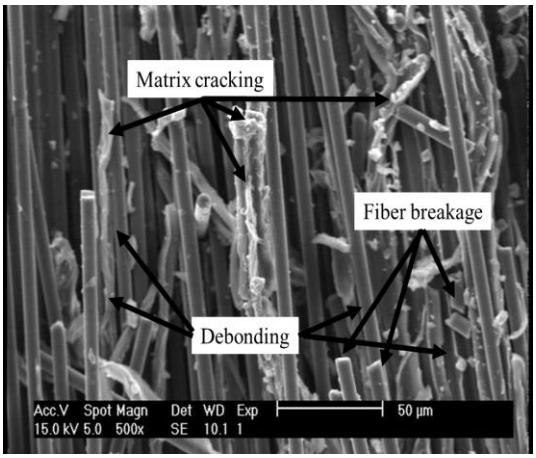

Fig. 9. The scanning electron microscopy image of damage mechanisms.

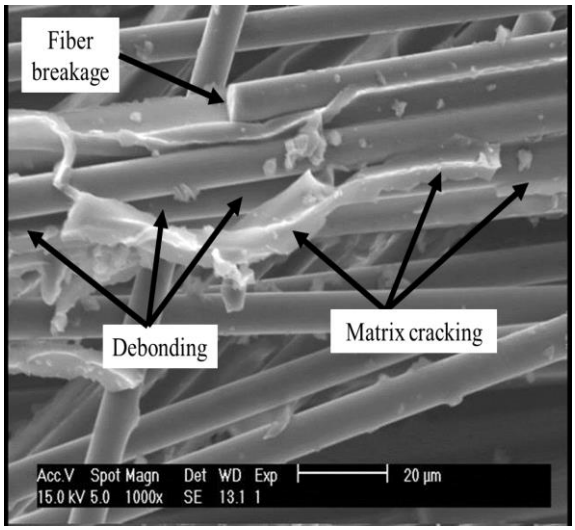

Fig. 10. The scanning electron microscopy image of damage mechanisms with higher magnification.

It should be noted that such obtained results, including three defect types in composite samples, were also represented similarly by the literature [11-14], under tensile monotonic and cyclic loadings, for the open-hole standard sample.

4. Conclusions

In this study, two different types of acoustic emission sensors were utilized to investigate the damage in composite samples during cyclic loading. Obtained results showed that both wide-band and mid-band sensors could be effectively used to monitor the health of composite structures. In addition, results clearly described the relationship between the stress history diagrams and acoustic energy parameters, including the energy, the count and the cumulative energy, for both two types of sensors. Scanning electron microscopy images showed that the damage mechanisms of the fiber breakage, matrix cracking and debonding of fibers from the matrix occurred in the composite specimen.

Acknowledgements

Authors of this article should thank Irankhodro Powertrain Company (IPCo.), for their financial support in conducting tests and using the acoustic emission equipments. In addition, authors want to thank Dr. M. Shakouri, for consulting in the manufacture of samples and Dr. S.A. Mousavian for consulting in analyzing the acoustic emission data and performing the tests.

References

[1] Liu PF, Chu JK, Liu YL, Zheng JY. A study on the failure mechanisms of carbon fiber/epoxy

composite laminates using acoustic emission. *Materials and Design* 2012; 37: 228–35.

[2] Mohammadi R, Najafabadi MA, Saeedifar M, Yousefi J, Minak G. Correlation of acoustic emission with finite element predicted damages in open-hole tensile laminated composites. *Composite Part B: Engineering* 2017; 108: 427–35.

[3] Fotouhi M, Ahmadi Najafabadi M. Investigation of the mixed-mode delamination in polymer-matrix composites using acoustic emission technique. *Journal of Reinforced Plastics and Composites* 2014; 33(19): 1767–82.

[4] Yousefi J, Ahmadi M, M. Shahri N, Oskouei AR, Moghadas FJ. Damage Categorization of Glass/Epoxy Composite Material under Mode II Delamination Using Acoustic Emission Data: A Clustering Approach to Elucidate Wavelet Transformation Analysis. *Arabian Journal of Science and Engineering* 2014; 39(2): 1325–35.

[5] Ni QQ, Iwamoto M. Wavelet transform of acoustic emission signals in failure of model composites. *Engineering Fracture Mechanics* 2002; 69(6): 717–28.

[6] Loutas TH, Kostopoulos V. Health monitoring of carbon/carbon, woven reinforced composites. Damage assessment by using advanced signal processing techniques. Part I: Acoustic emission monitoring and damage mechanisms evolution. *Composite Science and Technology* 2009; 69(2): 265–72.

[7] Nixon-Pearson OJ, Hallett SR, Withers PJ, Rouse J. Damage development in open-hole composite specimens in fatigue. Part 1: Experimental investigation. *Composite Structures* 2013; 106: 882–89.

[8] Bourchak M, Farrow IR, Bond IP, Rowland CW, Menan F. Acoustic emission energy as a fatigue damage parameter for CFRP composites. *International Journal of Fatigue* 2007; 29(3): 457–70.

[9] Williams RS, Reifsnider KL Investigation of Acoustic Emission During Fatigue Loading of Composite Specimens. *Journal of Composite Materials* 1974; 8(4): 340–55.

[10] Mahdavi HR, Rahimi GH, Farrokhabadi A. Failure analysis of (±55°)9 filament-wound GRE pipes using acoustic emission technique. *Engineering Failure Analysis* 2016; 62: 178–87.

[11] Sayar H, Azadi M, Ghasemi-Ghalebahman A, Jafari SM. Clustering effect on damage mechanisms in open-hole laminated carbon/epoxy composite under constant tensile loading rate, using acoustic emission. *Composite Structures* 2018; 204: 1-11.

[12] Alizadeh M, Azadi M, Farrokhabadi A, Jafari SM. Investigation of displacement amplitude effect on failure mechanisms in open-hole laminated composites under low-cycle fatigue loading using acoustic emission. *Modares Mechanical Engineering* 2018; 17(3): 435-45.

[13] Ghasemi-Ghalebahman A, Sayar H, Azadi M, Jafari SM. Failure mechanisms in open-hole laminated composites under tensile loading using acoustic emission. *Journal of Science and Technology of Composites* 2018; 5(1): 143-52.

[14] Azadi M, Sayar H, Ghasemi-Ghalebahman A, Jafari SM. Tensile loading rate effect on mechanical properties and failure mechanisms in open-hole carbon fiber reinforced polymer composite by acoustic emission approach. *Composite Part B: Engineering* 2019; 158: 448-58.

[15] Azadi M, Alizadeh M, Sayar H. Sensitivity analysis for effects of displacement amplitude and loading frequency on low-cycle fatigue lifetime in carbon/epoxy laminated composites. In: MATEC Web of Conferences (Fatigue 2018); 2018. 165: 22021.

[16] ASTM D5766 / D5766M - 11 Standard. **Test Method for Open-Hole Tensile Strength of Polymer Matrix Composite Laminates**. 2011.

[17] Beattie AG. Acoustic Emission, Principles and Instrumentation. *Journal of Acoustic Emission* 1983; 2: 95-128.

[18] ISO 12716. **Non-Destructive Testing - Acoustic Emission Inspection - Vocabulary**. 1998.

[19] Nakamura H, Ohtsu M, Enoki M, Mizutani Y, Shigeishi M, Inaba H, Nakano M, Shiotani T, Yuyama S, Sugimoto, S. **Practical Acoustic Emission Testing, Springer, Society for Non-Destructive Inspection**, Springer; 2016.

[20] Mix PE, **Introduction to Nondestructive testing: a training guide**. New York: Wiley; 2005.

[21] Grosse CU, Masayasu O. **Acoustic Emission Testing**. Springer; 2008.

[22] ASTM E976-10. **Standard Guide for Determining the Reproducibility of Acoustic Emission Sensor Response**. ASTM International: West Conshohocken; 2010.

[23] Roberts TM, Talebzadeh M. Acoustic emission monitoring of fatigue crack propagation. *Journal of Constructional Steel Research* 2003; 59: 695-712.

[24] Bassim MN, Lawrence SS, Liu CD. Detection of the onset of fatigue crack growth in rail steels using acoustic emission. *Engineering Fracture Mechanics* 1994; 47(2): 207-214.

[25] Harris DO, Dunegan HL. Continuous monitoring of fatigue-crack growth by acoustic-emission techniques. *Experimental Mechanics* 1974; 14: 71-81.

[26] Ma G, Li H. Acoustic emission monitoring and damage assessment of FRP-strengthened reinforced concrete columns under cyclic loading. *Construction and Building Materials* 2017; 144: 86-98